



HAL
open science

Impacts of environmental levels of hydrogen peroxide and oxyanions on the redox activity of MnO₂ particles

Daqing Jia, Qinzhi Li, Tao Luo, Olivier Monfort, Gilles Mailhot, Marcello Brigante, Khalil Hanna

► To cite this version:

Daqing Jia, Qinzhi Li, Tao Luo, Olivier Monfort, Gilles Mailhot, et al.. Impacts of environmental levels of hydrogen peroxide and oxyanions on the redox activity of MnO₂ particles. *Environmental Science: Processes & Impacts*, 2021, 9, 10.1039/D1EM00177A . hal-03321723

HAL Id: hal-03321723

<https://hal.science/hal-03321723v1>

Submitted on 31 Mar 2023

HAL is a multi-disciplinary open access archive for the deposit and dissemination of scientific research documents, whether they are published or not. The documents may come from teaching and research institutions in France or abroad, or from public or private research centers.

L'archive ouverte pluridisciplinaire **HAL**, est destinée au dépôt et à la diffusion de documents scientifiques de niveau recherche, publiés ou non, émanant des établissements d'enseignement et de recherche français ou étrangers, des laboratoires publics ou privés.

1 **Impacts of environmental levels of hydrogen peroxide and oxyanions on the**
2 **redox activity of MnO₂ particles**

3
4 Daqing Jia^a, Qinzhi Li^b, Tao Luo^b, Olivier Monfort^d, Gilles Mailhot^a, Marcello Brigante^a,
5 Khalil Hanna^{b,c*}

6 ^a *Université Clermont Auvergne, CNRS, Clermont Auvergne INP, Institut de Chimie de*
7 *Clermont-Ferrand, F-63000 Clermont-Ferrand, France.*

8 ^b *Univ. Rennes, École Nationale Supérieure de Chimie de Rennes, CNRS, ISCR UMR 6226, F-*
9 *35000 Rennes, France*

10 ^c *Institut Universitaire de France (IUF), MESRI, 1 rue Descartes, 75231 Paris, France.*

11 ^d *Comenius University in Bratislava, Faculty of Natural Sciences, Department of Inorganic*
12 *Chemistry, Ilkovicova 6, Mlynska Dolina, 842 15 Bratislava, Slovakia.*

13
14
15 *Corresponding author: +33 2 23 23 80 27, khalil.hanna@ensc-rennes.fr

20

21 **Abstract**

22 Despite the widespread presence of hydrogen peroxide in surface water and
23 groundwater systems, little is known about the impact of environmental levels of H₂O₂ on the
24 redox activity of minerals. Here we demonstrate that environmental concentrations of H₂O₂
25 can alter the reactivity of birnessite-type manganese oxide, an earth-abundant functional
26 material, and decrease its oxidative activity in natural systems across a wide range of pH
27 values (4-8). The H₂O₂-induced reductive dissolution generates Mn(II) that will re-bind to
28 MnO₂ surfaces, thereby affecting the surface charge of MnO₂. Bisphenol A (BPA), as a
29 ubiquitous environmental contaminant with endocrine disruption potential, was chosen to be
30 the target compound, while the competition of BPA and Mn(II) to interact with reactive
31 surface sites may cause suppression of the oxidative ability of MnO₂. This suppressive effect
32 becomes more effective in presence of oxyanions such as phosphate or silicate at
33 concentrations comparable to those encountered in natural waters. Unlike nitrate, adsorption
34 of phosphate or silicate onto birnessite increased in presence of Mn(II) added or generated
35 through H₂O₂-induced reduction of MnO₂. This suggests that naturally occurring anions and
36 H₂O₂ may have synergetic effects on the reactivity of birnessite-type manganese oxide at a
37 range of environmentally relevant H₂O₂ amounts. As layered structure manganese oxides play
38 a key role in the global carbon cycle as well as pollutant dynamics, the impact of
39 environmental levels of hydrogen peroxide (H₂O₂/MnO₂ molar ratio ≤ 0.3) should be
40 considered in environmental fate and transport models.

41

42

43 **Keywords:** birnessite; redox; hydrogen peroxide; oxyanion.

44

45

Table of contents

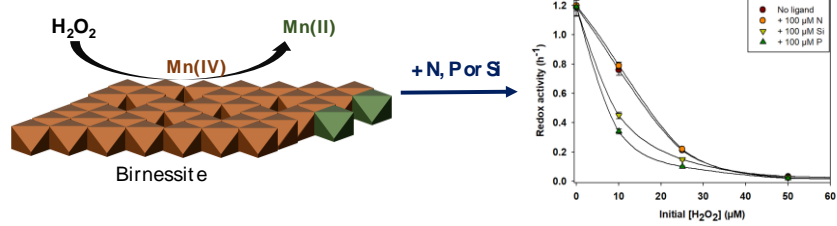
46

H_2O_2/MnO_2 molar ratio as low as 0.03 can affect the redox activity of MnO_2 particles and

47

their reactivity in natural systems.

48



49

50

51

52

53

54 **Introduction**

55 Layered structure manganese oxides (*e.g.* birnessite) are ubiquitous in a wide range of
56 aquatic and terrestrial environments.¹ The presence of exchangeable hydrated cations within
57 the interlayers combined with a high content of vacancy sites and variable oxidation states of
58 manganese make them powerful sorbents and oxidants.^{2,3} As a result, birnessite-type
59 manganese oxides play a significant role in controlling the cycles of several key nutrients as
60 well as the fate and mobility of inorganic and organic contaminants.⁴⁻⁹ Acid birnessite has
61 been widely investigated because it is structurally similar to biogenic “natural” manganese
62 oxides.¹⁰⁻¹³ The birnessite reactivity is mainly affected by solution pH, surface properties and
63 composition of MnO₂ and structural characteristics of contaminants (*i.e.*, BPA).^{4-6,12} It can
64 also be influenced by the presence of naturally occurring compounds, *e.g.* cations, anions,
65 natural organic matter and other redox-active compounds. Among the latter, hydrogen
66 peroxide (H₂O₂) has an ambivalent redox activity and is commonly found in aquatic
67 environments at concentration ranging from nM to μM.¹⁴⁻²⁶

68 In environmental systems, photodependent reactions mediated by natural organic matter
69 and biological-mediated processes dominate H₂O₂ production.²⁶ Sunlight-induced
70 photochemical reactions mediated by organic ligands and/or biochemical metabolic processes
71 can result in amounts of H₂O₂ up to 20 μM.¹⁴⁻¹⁸ Input from rainwater can reach up to 40 μM
72 ^{20,21}, while hydrogen peroxide production has been often observed in irradiated seawater.¹⁹⁻²¹
73 Light-independent generation of H₂O₂ has been recently reported in river sediments and in
74 groundwater of an alluvial aquifer, which is likely to occur in transitional redox environments
75 where reduced elements react with oxygen.^{22,23} For example, natural hydroquinones or
76 hydroquinone moieties ubiquitously present in reduced organic matter can donate electrons to
77 O₂ to generate H₂O₂.^{24,25} H₂O₂ production through microbial mechanism has also been shown
78 to enhance iodide oxidation and organo-iodine formation in soils and sediments.²⁷ All these

79 studies suggested that H_2O_2 can be formed not only in oceanic and atmospheric systems but
80 also in the subsurface environment. Finally, higher concentrations (up to 1 mM) have been
81 reported in nuclear waste repository scenarios when ionizing radiation of groundwater
82 adjacent to spent nuclear fuel result in H_2O_2 production.²⁸

83 Despite the catalyzed decomposition of hydrogen peroxide by MnO_2 has been well
84 investigated²⁹⁻³¹, knowledge is very limited on the effect of H_2O_2 on the reactivity of
85 birnessite at environmental levels of H_2O_2 . In engineering applications, metal oxides such as
86 MnO_2 are generally investigated for catalytic decomposition of H_2O_2 and then formation of
87 reactive transient species using very high concentrations of hydrogen peroxide (H_2O_2) (≥ 0.5
88 mM).²⁹⁻³¹ While these remediation studies aimed to eliminate pollution in contaminated
89 systems, they overlooked the influence of H_2O_2 on the electron transfer heterogeneous
90 reaction and then the oxidative activity of birnessite. In addition, little is known about the
91 influence of H_2O_2 on the birnessite composition and interactions of redox products (*e.g.*
92 Mn(II)) with MnO_2 surfaces.

93 In this study, we examine how H_2O_2 affects the reactivity of birnessite under
94 environmentally relevant conditions. To monitor H_2O_2 -induced changes in birnessite reactivity,
95 we used Bisphenol A (BPA) as a model compound because it has a strong reactivity with the
96 birnessite ($\delta\text{-MnO}_2$), with a well-documented underlying redox mechanism.³²⁻³⁵ Acid
97 birnessite, a well-established laboratory synthesized analog of layered birnessite mineral, was
98 chosen as a representative manganese dioxide mineral. The removal kinetics of BPA have
99 been assessed in presence of variable amounts of H_2O_2 under a wide range of pH (4, 6.5 and 8)
100 under aerobic and anaerobic conditions. Alteration of birnessite structure and composition
101 was monitored using XRD and titration experiments under different conditions ($\text{H}_2\text{O}_2/\text{MnO}_2$
102 molar ratio, dissolved Mn(II) amount and pH value). To check whether the impact of H_2O_2
103 can persist in natural waters, changes in birnessite reactivity were investigated in presence of

104 commonly found anionic ligands such as phosphate, nitrate and silicate. We notably
105 demonstrated that at H₂O₂ concentrations as low as 10 μM or with H₂O₂/MnO₂ molar ratio as
106 low as 0.03, the reactivity of acid birnessite can be affected, which could alter biogeochemical
107 cycles as well as pollutant dynamics.

108

109

110 **2. Materials and Methods**

111 **2.1. Chemicals**

112 KMnO₄ , HCl, NaCl, NaOH, HEPES, H₂C₂O₄, H₂SO₄, hydroxylamine hydrochloride,
113 H₂O₂, BPA, HNO₃, terephthalic acid, 2-hydroxyterephthalic acid, Na₂SiO₃, NaNO₃, NaH₂PO₄
114 and MnCl₂ were purchased from Sigma-Aldrich and were all AR grade. All chemicals were
115 used as received without further purification. All solutions were prepared in ultrapure water
116 obtained from a water purification system (Millipore, resistivity 18.2 MΩ cm).

117

118 **2.2. Synthesis and characterization of acid birnessite**

119 Acid birnessite was prepared following the procedure of McKenzie³⁶, and Mn(III)-rich
120 MnO₂ was synthesized according to previous published methods.^{37,38} More details are
121 provided in the Supporting Information (SI). The solid was characterized using X-ray powder
122 diffraction (XRD) using the Bruker AXS D8 Advance diffractometer (θ-2θ Bragg-Brentano
123 geometry) using monochromatized CuKα1 radiation over the range of 10°-100° 2θ at a step
124 size of 0.02°. X-ray diffraction (XRD) confirmed that the only product of the synthesis was
125 poorly-crystalline hexagonal birnessite. The Brunauer–Emmett–Teller (BET) specific surface
126 area of the synthetic birnessite measured by multipoint N₂ adsorption was 60 ± 2.5 (SD) m²
127 g⁻¹. The Average Oxidation State (AOS= 3.98 (±0.02)) of synthetic birnessite and (AOS=
128 3.65 (±0.02)) of Mn(III)-rich MnO₂ were measured using the oxalic acid-permanganate back-

129 titration method (more details are provided in SI). Scanning Electron Microscope (SEM;
130 JEOL JSM-7100F) and High-resolution Transmission Electron Microscope (HRTEM; JEOL
131 2100 LaB₆) images showed a nanoflower-shaped birnessite consisting of nanoflakes
132 aggregations (see Figure S1).

133 **2.3. Kinetics experiments and analyses**

134 Reactivity changes assessment were investigated as following: 100 mL aqueous
135 suspension of acid birnessite (AB) corresponding to an initial concentration of 345 μM was
136 first prepared and then an appropriate amount of stock solutions of H₂O₂, BPA, and/or Mn(II)
137 were added to start the reaction at room temperature. Since the involved reactions can
138 consume protons (see below), the pH was adjusted to the desired value and then kept constant
139 throughout the reaction using a pH meter (Cyberscan 510, Thermo Scientific) by adding 0.1
140 M NaOH or HCl. The suspension was stirred at an agitation speed of 350 rpm during the
141 experiments. 1 mL of aqueous sample was withdrawn at different time interval, filtered
142 through 0.22 μm PTFE filter, and then analyzed. The same batch experiments were carried out
143 in the presence of silicate and phosphate to test the effect of anions and H₂O₂ on BPA
144 oxidation.

145 Potential generation of hydroxyl radical was monitored through the fluorescence emission
146 spectrum of 2-hydroxyterephthalic acid (λ_{ex} 320 nm, λ_{em} 425 nm) using a spectrofluorometer
147 (Shimadzu RF-5301PC) (more information at SI).

148 The BPA concentration was determined by a high-performance liquid chromatography
149 system (HPLC, Waters Alliance) equipped with a diode array detector (DAD).
150 Chromatographic separation was performed using a Nucleodur 100-5 C18 column (150 \times 4.6
151 mm, 5 μm of particle size, Macherey Nagel). The detection wavelength of BPA was set at 277
152 nm and the column temperature was kept at 30 $^{\circ}\text{C}$. Methanol and water were mixed as the
153 mobile phase under a gradient eluent mode, and the percentage of methanol changed with

154 time was as follows: from 0 to 7 min was increased from 70 to 90% and kept constant up to 9
155 min. The flow rate was set at 0.8 mL min⁻¹. The byproducts of BPA oxidation were identified
156 using Ultraperformance Liquid Chromatography-tandem Mass Spectrometry (UPLC-MS/MS)
157 system. An electrospray interface was used for the MS measurements in positive ionisation
158 mode and full scan acquisition.

159 H₂O₂ concentration was determined using a spectrofluorometric detection as described in
160 our previous work.³⁹ Briefly, samples containing H₂O₂ were mixed with 4-
161 hydroxyphenylacetic acid to form the stable 4-hydroxyphenyl acetic acid dimer in the
162 presence of peroxidase (POD, Sigma-Aldrich). The 4-hydroxyphenylacetic acid dimer was
163 quantified using a Cary Eclipse fluorescence spectrophotometer. The excitation wavelength
164 was set at 320 nm and emission wavelength maximum was determined at 420 nm.
165 Concentration was calculated using calibration curve obtained using different concentrations
166 of H₂O₂.

167 Dissolved Mn(II) concentration in aqueous solution was determined by Atomic
168 Absorption Spectroscopy (AAS, PerkinElmer). All the samples were first filtered using a
169 PTFE 0.22 µm filter and then mixed with 2% nitric acid (HNO₃, 65%, Sigma- Aldrich) prior
170 for analyses. Dissolved Mn(II) standard solution for AAS (TraceCERT®, 1000 mg L⁻¹ Mn(II)
171 in 2% nitric acid, Sigma-Aldrich) was used for the calibration curve. The detection
172 wavelength was set at 279 nm and the AAS detection limit is below 0.02 µM. Mn(II) removal
173 was calculated as the difference between the initial and final Mn(II) solution concentrations.

174 The impact of anions on reactivity changes was investigated as mentioned above, but with
175 addition of the chosen anion with BPA or Mn(II) to the AB suspension. Silicate concentration
176 was determined by the molybdenum-blue colorimetric method⁴⁰ while phosphate and nitrate
177 concentrations by ion chromatography.⁴¹ XRD was performed to determine the possible
178 transformation of solids upon Mn(II) sorption.

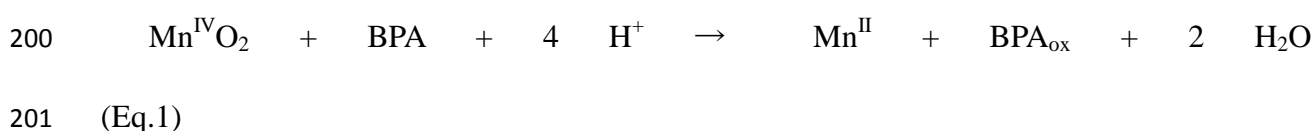
179 Since Mn(II) oxidation by molecular oxygen may take place, particularly at alkaline pH
180 values, we compared the removal kinetics under aerobic (open atmosphere) vs anaerobic
181 conditions (glove box N₂:H₂ 98:2). Ultrapure water under anoxic environments were sparged
182 with nitrogen to remove oxygen prior to use. These preliminary tests showed that there is no
183 effect of oxic conditions on the BPA removal in presence of H₂O₂ or Mn(II). Great attention
184 has also been paid to the pH adjustment in all experiments, since the involved reactions are
185 sensitive to pH value (see below). All experiments were conducted in triplicates and the
186 standard deviation was calculated for all experimental series.

187

188 **3. Results and Discussion**

189 **3.1 Effect of H₂O₂ on the oxidative ability of birnessite**

190 BPA removal was monitored in the presence of acid birnessite (AB) at different H₂O₂
191 concentrations at pH 6.5 (Fig. 1). In the absence of H₂O₂, almost complete removal of BPA
192 was observed after 24h of reaction time. Mass balance showed that the oxidation reaction was
193 mainly involved in the removal of BPA in presence of MnO₂, while adsorption was very low
194 under our experimental conditions (*i.e.* less than 5% of initial BPA), which is consistent with
195 previous investigations.^{6,32,33} Indeed, BPA containing two hydroxyphenyl functionalities is
196 known to weakly interact with mineral surfaces, resulting in lower adsorption affinity to
197 metal-oxides.³² As previously reported,^{6,33,42} binding to birnessite is followed by an electron
198 transfer process resulting in the concomitant oxidation of sorbed compound and reduction of
199 surface-bound Mn(IV) to yield Mn(III) that can be further reduced to give Mn(II).



202 Electron exchange of BPA with MnO₂ form a radical, followed by a series of reactions
203 including radical coupling, fragmentation, substitution and elimination to form multiple

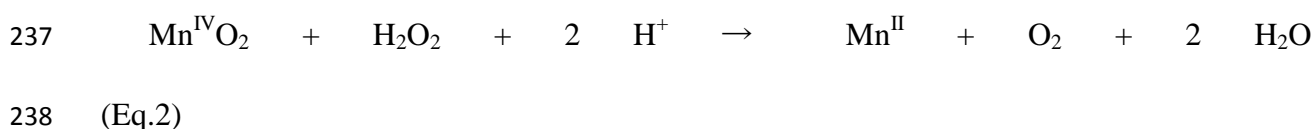
204 byproducts.^{6,32,33} LC/MS analysis identified one predominant species of mass-to-charge ratio
205 of $m/z = 135$ as the most dominant byproduct of BPA over the first reaction time (90 min),
206 which likely corresponds to 4-hydroxycumyl alcohol according to previous investigations.⁴³

207 In the presence of hydrogen peroxide, the oxidative removal of BPA gradually decreased
208 with increasing in H_2O_2 concentration, and completely suppressed at higher dose of H_2O_2
209 (200 μM equivalent to a H_2O_2/MnO_2 molar ratio ~ 0.6). In these experiments, the H_2O_2
210 decomposition is relatively fast whatever the investigated pH, since complete decomposition
211 of H_2O_2 was achieved after 15 min of reaction, even for the highest H_2O_2 dose (See Fig. S2
212 and S3). Monitoring of fluorescence emission spectra of suspensions using a terephthalate as
213 a chemical probe indicated that no hydroxyl radical was generated under the experimental
214 conditions of this study. Additional experiments using 1-propanol and t-butanol as hydroxyl-
215 radical scavengers confirmed that the BPA removal is a no radical-based oxidation process
216 regardless of the presence or absence of H_2O_2 .

217 The suppressive effect of H_2O_2 on the removal rate of BPA was then confirmed at two
218 other pH values (4 and 8). The removal kinetics could not be properly described by simple
219 equations that include classical exponential functions (*e.g.*, first- or second- order model),
220 probably due to the complexity of involved reactions in the investigated system. Instead, we
221 calculated the initial rate constant (k, h^{-1}) by linear regression of $\ln [BPA]/[BPA]_0$ versus time
222 over the first stage of reaction (*i.e.*, 60 min). The initial rate constants for all investigated
223 H_2O_2 amounts exhibited the same order, $pH\ 4 > pH\ 6.5 > pH\ 8$ (Fig. 2). In the absence of
224 H_2O_2 , k was decreased almost 20-fold when pH increased from 4 to 8. This suggests that
225 acidic conditions favored BPA removal, a trend also observed for other organic compounds
226 reacting with MnO_2 .^{33,34,44} We attribute this to variability in two pH-dependent factors: 1)
227 speciation of BPA that affects binding to MnO_2 surfaces and then oxidation (Fig. S4), and 2)
228 redox-potential of MnO_2 that decreases when the pH increased from 4 to 8.⁴⁵ At relatively

229 low pH, favorable electrostatic interactions between neutral BPA molecules and the negatively
230 charged surface of MnO₂ (PZC of MnO₂ is ~ 2.3-2.9) may exist. On the other hand, reductive
231 conversion of MnO₂ into Mn(II) is dependent on the amount of protons, which would result
232 in increase in BPA removal rate when the pH decreases (Eq.1). In the presence of H₂O₂, the
233 removal rate constants of BPA sharply decreased with increasing in H₂O₂ amount whatever
234 the investigated pH value (Fig. 2).

235 As for BPA, it is previously reported that hydrogen peroxide can also reduce Mn(IV) to
236 Mn(III) and then Mn(II) as follows^{46,47} :



239 To check this possibility under our experimental conditions, the reductive dissolution of
240 MnO₂ in presence of various amounts of H₂O₂ was monitored at three pH values (Fig. 3). In
241 both Eq.1 and Eq.2, protons are directly involved in the oxidation of BPA as well as the
242 reductive dissolution of MnO₂. In the absence of H₂O₂, dissolved Mn(II) was only detected at
243 pH 4, while it was below the detection limit at pH 6.5 or 8. Increasing H₂O₂ concentration
244 from 50 μM to 200 μM enhanced the amount of dissolved Mn(II), at the three investigated pH
245 values. At each pH value, the amount of dissolved Mn(II) increased first, reached a maximum
246 and then decreased. This two-step behavior is consistent with the H₂O₂ decomposition over
247 time, where the complete decomposition of H₂O₂ observed after approximately 15 min of
248 reaction time coincides with the peak observed for dissolved Mn(II) generation (Fig. S3).
249 Once the added H₂O₂ is fully decomposed, the generated dissolved Mn(II) will in turn sorb
250 onto MnO₂ surfaces. Because higher pH implies more Mn(II) binding⁴⁸⁻⁵⁰, greater amounts of
251 Mn(II) were observed at low pH values (Fig. 3). When a further addition of H₂O₂ is made
252 after total decomposition of the initial amount (*e.g.* after 15 min at pH 4), the amount of
253 generated Mn(II) increased again and reached almost twice the first measured amount within

254 approximately 15 min (not shown). This suggests that the reductive dissolution of MnO₂ by
255 H₂O₂ is a fast process, as compared to the reaction between MnO₂ and BPA.

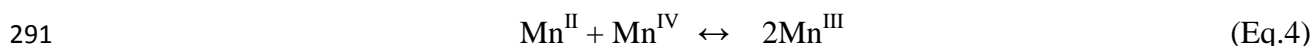
256

257 To check whether Eq.1 and Eq.2 may occur simultaneously during the heterogeneous
258 reactions with MnO₂, we compare the standard potential of involved reactions at the working
259 pH range. MnO₂ has standard (reduction) potential varying from 0.99 to 0.76 V when the pH
260 rises from 4 to 8 for MnO₂ + 4 H⁺ + 2 e⁻ → Mn^{II} + 2 H₂O. This value is higher than the
261 standard oxidation potential of O₂/H₂O₂ (O₂ + 2 H⁺ + 2e⁻ → H₂O₂ 0.68 V vs. NHE) or of BPA
262 which varies between 0.75 V and 0.52 V in the pH range 4-8.⁵¹⁻⁵³ Since the latter redox
263 couples have comparable oxidation potential, reactions (Eq.1) and (Eq.2) could
264 simultaneously take place. Assuming that these reactions obey pseudo-first order kinetic
265 equation because MnO₂ is considered in excess, the reaction rate depends on the
266 concentration of reactants (*i.e.* H₂O₂ or BPA). When the H₂O₂ amount increases, the reaction
267 2 should become much faster than the reaction 1. This was experimentally shown in Figures 1
268 and 3 and Figure S3, where both reactions Eq.1 and Eq.2 occurred simultaneously until
269 complete inhibition of Eq.1 at the highest H₂O₂ amount (200 μM). Though H₂O₂ was full
270 decomposed after 15 min of reaction time (Fig. S2), the suppressive effect on the birnessite
271 reactivity was still observed over 24 h of reaction time (Fig. 1). This was confirmed by
272 carrying out sequentially the reactions (Eq.2) and (Eq.1). Indeed, suppression of BPA removal
273 capacity was also observed when MnO₂ and H₂O₂ were allowed to react first (*i.e.* pre-
274 equilibration step of 30 min) until total decomposition of H₂O₂ before addition of BPA (not
275 shown). Therefore, the H₂O₂-mediated reduction of MnO₂ (Eq.2) considerably affects the
276 surface reactivity of birnessite and its ability to remove BPA. This reductive dissolution
277 generates Mn(II) ions which will in turn bind to MnO₂ surfaces and then be oxidized into
278 higher valence Mn:



280 This oxidation reaction may be made possible by the residual H_2O_2 and/or generated O_2
281 (through Eq.2), which is pH-dependent. The contribution of O_2 from ambient air is excluded
282 since reactivity assessment tests investigated under aerobic vs anaerobic conditions showed
283 similar behavior in term of BPA removal.

284 It is worth noting that strong aggregation of MnO_2 particles and then fast sedimentation
285 was observed upon addition of H_2O_2 . This phenomenon can be ascribed to charge
286 neutralization (*i.e.* surface charge switch from negative to positive) upon $\text{Mn}(\text{II})$ ions binding
287 to negatively charged MnO_2 surfaces, as previously reported.⁵⁴ Furthermore,
288 disproportionation/comproportionation reaction (Eq.4) may occur within the MnO_2 , *i.e.* Mn^{II}
289 exchanges electrons with $\text{Mn}(\text{IV})$ to form two $\text{Mn}(\text{III})$ centers and, conversely, two $\text{Mn}(\text{III})$
290 centers can disproportionate to form $\text{Mn}(\text{II})$ and $\text{Mn}(\text{IV})$ centers^{12,32,35,50,55}:



292 Since this reaction is pH-dependent, we have measured the average oxidation state (AOS)
293 of birnessite over the whole investigated pH range (4-8). The AOS of samples reacted with
294 BPA (25 μM) alone only slightly decreased from 3.98 to 3.90 (± 0.02). However, partial
295 reduction of MnO_2 upon addition of 200 μM of H_2O_2 dropped down the AOS to 3.74 (± 0.04)
296 at pH 4 and 6.5, and 3.61 (± 0.04) at pH 8. This decrease suggests that percentages of $\text{Mn}(\text{III})$
297 or $\text{Mn}(\text{II})$ or both are relatively higher at the end of reaction with respect to the initial sample.
298 The formation of $\text{Mn}(\text{III})$ was further confirmed by the detection of $\text{Mn}(\text{III})$ -pyrophosphate
299 complex at 480 nm, $\text{Mn}(\text{III})$ being stabilized through ligand-binding complexes.⁵⁶ The effect
300 of H_2O_2 on the structure of birnessite will be discussed in the following section.

301 Collectively, these results suggest that the H_2O_2 induced reduction of MnO_2 is an effective
302 process, and the fast generation of $\text{Mn}(\text{II})$ is key for suppressed oxidative capacity of MnO_2
303 towards BPA. To confirm the impact of $\text{Mn}(\text{II})$ on the reactivity of MnO_2 , BPA removal

304 kinetics were investigated in Mn(II)-amended birnessite suspensions in the following section.

305

306 **3.2. Effects of Mn(II) on the removal capacity of MnO₂**

307 The initial rate constants of BPA removal sharply decreased with increasing in dissolved
308 Mn(II) amount at pH 4 and 6.5, while at pH 8 it increased first between 0 and 10 μM but later
309 decreased with increasing in initial Mn(II) amount (Fig. 5). It is previously reported that the
310 adsorption of cations such as Ca(II) or Mg(II) may change the surface charge from negative
311 to positive by exchange of H^+ on the MnO_2 surface.^{57,58} Similarly, the Mn(II) adsorption
312 should lead to a decrease in the negative surface charge, thereby altering the binding capacity
313 of MnO_2 . When the Mn(II) amount further increases, we speculate a competition between
314 BPA and Mn(II) to bind at reactive sites of MnO_2 during the first kinetic phase, as recently
315 observed for quinolones.⁴²

316 As for H_2O_2 , dissolved Mn(II) displayed suppressive effects on the removal rate of BPA
317 and the rate constants over the whole Mn(II) concentration range (10 - 100 μM) exhibited the
318 same order, pH 4 > pH 6.5 > pH 8 (Fig. 5). In addition to the comproportionation reaction that
319 is pH-dependent, the decrease in the oxidative ability of MnO_2 in the presence of dissolved
320 Mn(II) may result from competition of compound and Mn(II) to interact with reactive surface
321 sites. The strong binding of Mn(II) to MnO_2 surfaces suggests competition of BPA and Mn(II)
322 for surface sites, which is pH dependent.^{33,44} Dissolved Mn(II) measurements showed that
323 complete removal of dissolved Mn(II) was observed at both pH 6.5 and 8 when 100 μM
324 Mn(II) was used (not shown), while a concentration of $\sim 30 \mu\text{M}$ was still measured at pH 4.

325 To check the affinity of birnessite for Mn(II) binding, sorption isotherms were
326 determined at three pH values (4, 6.5 and 8) under aerobic conditions (Fig. S5). It should be
327 noted that Mn(II) removal under oxic conditions is expected to be higher than under anoxic
328 conditions, especially at alkaline pH values, which has been attributed to surface-catalyzed

329 oxidation of Mn(II) by molecular oxygen.^{48,49} Here, only aerobic conditions were tested, since
330 the aim of these sorption isotherms is to assess the Mn(II) affinity under oxidizing conditions
331 imposed by the presence of H₂O₂. As expected, Mn(II) binding to MnO₂ surfaces increased
332 with pH increasing. Sorption isotherms showed different shape depending on pH value across
333 the Mn(II) concentration range. At pH 4 a typical L-shape with a plateau was observed, while
334 the removal amount continuously increased with Mn(II) concentration at higher pH values.
335 This high binding of Mn(II) at high pH value could cause Mn(III) enrichment in MnO₂
336 surfaces.^{48,49} Some studies have shown that at high Mn(II)/Mn(IV) ratio and pH > 7.5,
337 dissolved Mn(II) can interact with hexagonal birnessite and then transfer electron to lattice
338 Mn(IV) producing Mn(III).^{48,49} The buildup of Mn(III) will induce changes in mineral
339 structure and composition by converting birnessite into lower-valence Mn phases. XRD
340 analysis conducted on samples reacted with 100 μM of dissolved Mn(II) (Mn(II)/MnO₂ molar
341 ratio = 0.3) showed no notable transformation of MnO₂ over the investigated pH range (Fig.
342 4). However, titration experiments showed that addition of 100 μM of dissolved Mn(II)
343 dropped down the AOS of MnO₂ from 3.98 to 3.60 (±0.05) at pH 4 and 6.5, and 3.50 (±0.05)
344 at pH 8, suggesting more Mn(III) or Mn(II) at the end of reaction with respect to the initial
345 sample. A recent work showed that birnessite transformation into triclinic birnessite and/or 4
346 × 4 tunneled Mn oxide may occur at low Mn(II)/MnO₂ ratios (0.09 and 0.13), while
347 secondary phases such as MnOOH and Mn₃O₄ can be generated at high Mn(II)/MnO₂ ratios
348 (0.5 and 1).⁵⁹ In our XRD patterns, broad bands (hump) have appeared between 12° and 22°
349 and between 25° and 35° in the samples reacted with Mn(II) (Mn(II)/MnO₂ molar ratio = 0.3)
350 or H₂O₂ (H₂O₂/MnO₂ molar ratio = 0.6), suggesting changes in the structure or ordering of the
351 birnessite mineral sheets (Fig. 4). We also observed these broad bands in the XRD pattern of
352 synthetic Mn(III)-rich birnessite sample (see Fig. 4). This is consistent with previous studies,
353 which suggested that Mn^{III} formation can be made in edge-sharing complexes on MnO₂ edge

354 sites or around vacancy sites in octahedral layers of MnO₂.⁵ In addition, a small peak near 20°
355 only present in the patterns of samples reacted at pH 8 would suggest the presence of
356 feitknechtite (β-MnOOH), as previously reported.⁴⁸

357

358 **3.3. Synergistic effects of anions and H₂O₂ on the oxidative activity of MnO₂**

359 To check whether the suppression of reactivity at environmental relevant
360 concentrations of H₂O₂ can persist in presence of naturally occurring compounds, the initial
361 rate constants k (h⁻¹) of BPA removal were determined at pH 6.5 in presence of silicate, nitrate
362 and phosphate, commonly found in natural systems (Fig. 6). At 0 μM of H₂O₂, the presence of
363 100 μM of anions did not significantly influence the removal rate of BPA, probably because
364 of weaker interactions of these anionic ligands with MnO₂ surfaces under the experimental
365 conditions of this study (pH 6.5, 100 μM of anion, 345 μM of MnO₂). However, significant
366 decrease in kinetic rate constants was observed in presence of silicate and phosphate when
367 H₂O₂ was added in the reaction medium (H₂O₂/MnO₂ molar ratio between 0.03 and 0.3),
368 while no impact on the reactivity was observed in presence of nitrate (Fig. 6). These results
369 can be explained if the H₂O₂-mediated reduction of MnO₂ into Mn(II) make the presence of
370 silicate or phosphate competitive towards BPA interactions with MnO₂ surfaces. This was
371 confirmed by repeating removal kinetics of BPA in presence of 100 μM silicate or phosphate,
372 but with the addition of Mn(II) instead of H₂O₂ (data not shown). This suggests that presence
373 of Mn(II) added or generated through H₂O₂-mediated reduction renders the MnO₂ surfaces
374 more able to bind anionic ligands, thereby altering surface reactivity.

375 It is previously reported that unlike nitrate, silicate or phosphate may interact with
376 MnO₂ through hydrogen bonding or formation of outer-sphere complexes with surface
377 hydroxyl groups of MnO₂.⁵⁸⁻⁶¹ On the other hand, previous studies reported that the presence
378 of dissolved silicate may decrease the oxidation rate constants of MnO₂ toward chlorinated

379 compounds.^{62,63} They have attributed the decrease in MnO₂ reactivity to the surface-bound
380 silicate but none of them have provided adsorption data of silicate onto MnO₂. In the present
381 work, we showed that silicate or phosphate has a very low affinity to the negatively charged
382 MnO₂ surfaces under our experimental conditions, but the presence of 100 μM of Mn(II)
383 significantly enhanced their adsorption amounts onto MnO₂ (Fig. S6). This increased
384 adsorption might be due to the changes in both the surface charge of MnO₂ and the solution
385 speciation of anionic ligands in the presence of divalent cations such as Mn(II). Indeed, the
386 ligand speciation may be modified, since different coordination modes of aqueous complexes
387 of phosphate with Mn(II) ions have been previously reported.⁶⁴ However, no precipitation is
388 possible under our experimental conditions due to the low degree of saturation, *i.e.* low
389 aqueous concentration of free Mn(II) or ligand ($\log K_s \text{ Mn(II)/phosphate} = -27.07$).⁶⁵
390 Furthermore, Mn(II) binding should lead to a decrease in the negative surface charge, thereby
391 enhancing ability to bind anions through electrostatic interactions.^{54,57,58} Therefore, the MnO₂-
392 bound Mn(II) system could adsorb more effectively anions such as phosphate or silicate
393 through cation bridging, as recently reported for humic acid.⁵⁴ This surface-Mn(II)-ligand
394 ternary complex may act as a barrier to electron transfer between BPA and Mn(IV) sites,
395 thereby altering reactivity of MnO₂ surfaces.

396 It should be noted that silicate or phosphate (100 μM) did not significantly affect the
397 decomposition rate of H₂O₂ (200 μM), since total decomposition was achieved after
398 approximately 15 min as previously observed in Figure S2. Previous works have investigated
399 the catalytic activity of manganese oxides for hydrogen peroxide decomposition and
400 generation of reactive oxygen species in the context of environmental remediation studies.²⁹⁻³¹
401 Despite silicate adsorption on MnO₂ surfaces was found negligible, the effect of silicate
402 concentration (ranging from 0 to 1.5 mM) on the H₂O₂ decomposition rate has been found to
403 display relatively inhibition.³⁰ Although these works have used different experimental

404 conditions (*e.g.* much higher concentration of ligands or H₂O₂), and different MnO₂ types, the
405 present findings call for in-depth consideration of the combined/synergistic effects that the
406 cations and anions co-presents in the reaction medium may have on the MnO₂ reactivity.
407 Overall, these findings suggest that Mn(II) generation through H₂O₂-mediated reduction may
408 alter both adsorption and redox transformation of environmental compounds.

409

410 **4. Conclusions**

411 Photochemical and dark production of H₂O₂ make it ubiquitous not only in oceanic
412 and atmospheric systems but also in the subsurface environment. Here, we have notably
413 demonstrated that environmental levels of hydrogen peroxide can induce reductive dissolution
414 of MnO₂ into Mn(II), thereby affecting the surface reactivity of MnO₂. As the H₂O₂
415 decomposition is a fast process, the generated dissolved Mn(II) binds to MnO₂ surfaces,
416 altering further interactions with co-existing organic compounds. This may result from
417 competition of organic compound and Mn(II) to interact with reactive surface sites and/or
418 aqueous complexation with Mn(II). The presence of silicate or phosphate at concentrations
419 comparable to those encountered in natural waters further decreased the reactivity of MnO₂ in
420 presence of H₂O₂. Birnessite-bound Mn(II) adsorbed more effectively anionic ligands such as
421 phosphate or silicate and thus reducing interactions with BPA at a range of environmentally
422 relevant pH values. These findings suggest that naturally occurring anions and H₂O₂ may
423 have synergetic effects on the reactivity of nanostructured birnessite-type manganese oxide.
424 As manganese oxides can break down high molecular weight humic substances into lower
425 molecular weight organic molecules and/or stabilize dissolved organic carbon, these findings
426 call for in-depth consideration of the impacts of environmental levels of H₂O₂ and co-existing
427 anions on the global carbon cycle. Furthermore, the widespread presence of H₂O₂ in surface

428 and ground water systems and associated impacts on the redox-active minerals should be
429 considered in contaminant fate and transport assessment.

430

431 **Conflicts of interest**

432 There are no conflicts to declare.

433

434 **Acknowledgments**

435 This work was supported by the Institut Universitaire de France, the Region Council of
436 Auvergne Rhône-Alpes and the CNRS. We gratefully acknowledge the Chinese Scholarship
437 Council of PR China for providing financial support for Daqing Jia and Qinzhi Li.

438

439 **Supplementary Material**

440 Additional information regarding synthesis and characterization methods, SEM/TEM images,
441 additional data on removal kinetics and H₂O₂ decomposition, anions speciation and
442 adsorption onto MnO₂.

443

444 **Reference**

- 445 1 J. E. Post, Manganese oxide minerals: Crystal structures and economic and environmental significance,
446 *Proc. Natl. Acad. Sci.*, 1999, **96**, 3447-3454.
- 447 2 Y. Wang, S. Benkaddour, F. F. Marafatto and J. Peña, Diffusion-and pH-dependent reactivity of layer-
448 type MnO₂: Reactions at particle edges versus vacancy sites, *Environ. Sci. Technol.*, 2018, **52**, 3476-
449 3485.
- 450 3 N. Birkner and A. Navrotsky, Thermodynamics of manganese oxides: Sodium, potassium, and calcium
451 birnessite and cryptomelane, *Proc. Natl. Acad. Sci. U.S.A.*, 2017, **114**, E1046-E1053.
- 452 4 S. Wick, J. Peña and A. Voegelin, Thallium sorption onto manganese oxides, *Environ. Sci. Technol.*,
453 2019, **53**, 13168–13178.
- 454 5 B. J. Lafferty, M. Ginder-Vogel, M. Zhu, K. J. Livi and D. L. Sparks, Arsenite oxidation by a poorly
455 crystalline manganese-oxide. 2. Results from X-ray absorption spectroscopy and X-ray diffraction,
456 *Environ. Sci. Technol.*, 2010, **44**, 8467-8472.
- 457 6 C. K. Remucal and M. Ginder-Vogel, A critical review of the reactivity of manganese oxides with
458 organic contaminants, *Environ. Sci. Process. Impacts.*, 2014, **16**, 1247–1266.
- 459 7 R. Pokharel, Q. Li, L. Zhou and K. Hanna, Water flow and dissolved Mn(II) alter transformation of
460 pipemidic acid by manganese oxide, *Environ. Sci. Technol.*, 2020, **54**, 8051-8060.
- 461 8 J. Huang and H. Zhang, Redox reactions of iron and manganese oxides in complex systems, *Front.*
462 *Environ. Sci. Eng.*, 2020, 14, 76.
- 463 9 A. N. Ricko, A. W. Psoras and J. D. Sivey, Reductive transformations of dichloroacetamide safeners:
464 effects of agrochemical co-formulants and iron oxide manganese oxide binary-mineral systems,
465 *Environ. Sci.: Processes Impacts.*, 2020, **22**, 2104-2116.
- 466 10 M. Villalobos, B. Lanson, A. Manceau, B. Toner and G. Sposito, Structural model for the biogenic Mn
467 oxide produced by *Pseudomonas putida*, *Am. Mineral.*, 2006, 91, 489-502.
- 468 11 S. M. Webb, B. M. Tebo and J. R. Bargar, Structural characterization of biogenic Mn oxides produced
469 in seawater by the marine bacillus sp. strain SG-1, *Am. Mineral.*, 2005, 90, 1342-1357.
- 470 12 M. Zhu, M. Ginder-Vogel, S. J. Parikh, X.-H. Feng and D. L. Sparks, Cation effects on the layer
471 structure of biogenic Mn-oxides, *Environ. Sci. Technol.*, 2010, 44, 4465-4471.

- 472 13 M. Villalobos, B. Toner, J. Bargar and G. Sposito, Characterization of the manganese oxide produced by
473 *Pseudomonas putida* strain MnB1, *Geochim. Cosmochim. Acta.*, 2003, 67, 2649-2662.
- 474 14 W. J. Cooper and D. R. Lean, Hydrogen peroxide concentration in a northern lake: Photochemical
475 formation and diel variability, *Environ. Sci. Technol.*, 1989, 23, 1425–1428.
- 476 15 R. G. Zika, J. W. Moffett, R. G. Petasne, W. J. Cooper and E. S. Saltzman, Spatial and temporal
477 variations of hydrogen peroxide in gulf of Mexico waters, *Geochim. Cosmochim. Acta.*, 1985, 49,
478 1173–1184.
- 479 16 B. Gonzalez-Flecha and B. Demple, Homeostatic regulation of intracellular hydrogen peroxide
480 concentration in aerobically growing, *Escherichia Coli*. *J. Bacteriol.*, 1997, 179, 382–388.
- 481 17 F. Guillén, A. T. Martinez and M. J. Martínez, Production of hydrogen peroxide by aryl-alcohol oxidase
482 from the ligninolytic fungus *Pleurotus Eryngii*, *Appl. Microbiol. Biotechnol.*, 1990, 32, 465–469.
- 483 18 S. Garg, A. L. Rose and T. D. Waite, Photochemical Production of Superoxide and Hydrogen Peroxide
484 from Natural Organic Matter, *Geochim. Cosmochim. Acta.*, 2011, 75, 4310–4320.
- 485 19 J. W. Moffett and O. C. Zajiriou, An investigation of hydrogen peroxide chemistry in surface waters of
486 vineyard sound with $H_2^{18}O_2$ and $^{18}O_2$, *Limnol. Oceanogr.*, 1990, 35, 1221–1229.
- 487 20 K. L. Roe, R. J. Schneider, C. M. Hansel and B. M. Voelker, Measurement of dark, particle-generated
488 superoxide and hydrogen peroxide production and decay in the subtropical and temperate North
489 Pacific Ocean, *Deep Sea Res. Part I Oceanogr. Res. Pap.*, 2016, 107, 59–69.
- 490 21 W. J. Cooper, J. K. Moegling, R. J. Kieber and J. J. Kiddle, A chemiluminescence method for the
491 analysis of H_2O_2 in natural waters, *Mar. Chem.*, 2000, 70, 191–200.
- 492 22 X. Yuan, P. S. Nico, X. Huang, T. Liu, C. Ulrich, K. H. Williams and J. A. Davis, Production of
493 hydrogen peroxide in groundwater at rifle, Colorado, *Environ. Sci. Technol.*, 2017, 51, 7881–7891.
- 494 23 P. Liao, K. Yu, Y. Lu, P. Wang, Y. Liang and Z. Shi, Extensive dark production of hydroxyl radicals
495 from oxygenation of polluted river sediments, *Chem. Eng. J.*, 2019, 368, 700–709.

- 496 24 E. Kim, Y. Liu, C. J. Baker, R. Owens, S. Xiao, W. E. Bentley and G. F. Payne, Redox-cycling and
497 H₂O₂ generation by fabricated catecholic films in the absence of enzymes, *Biomacromolecules.*,
498 2011, 12, 880–888.
- 499 25 S. E. Page, G. W. Kling, M. Sander, K. H. Harrold, J. R. Logan, K. McNeill and R. M. Cory, Dark
500 Formation of hydroxyl radical in arctic soil and surface waters, *Environ. Sci. Technol.*, 2013, 47,
501 12860–12867.
- 502 26 J. D. Begg, M. Zavarin and A. B. Kersting, Plutonium desorption from mineral surfaces at
503 environmental concentrations of hydrogen peroxide, *Environ. Sci. Technol.*, 2014, 48, 6201-6210.
- 504 27 H.-P. Li, C. M. Yeager, R. Brinkmeyer, S. Zhang, Y.-F. Ho, C. Xu, W. L. Jones, K. A. Schwehr, S.
505 Otsuka and K. A. Roberts, Bacterial production of organic acids enhances H₂O₂-dependent iodide
506 oxidation, *Environ. Sci. Technol.*, 2012, 46, 4837–4844.
- 507 28 M. Amme, W. Bors, C. Michel, K. Stettmaier, G. Rasmussen and M. Betti, Effects of Fe(II) and
508 hydrogen peroxide interaction upon dissolving UO₂ under geologic repository conditions, *Environ.*
509 *Sci. Technol.*, 2005, 39, 221–229.
- 510 29 R. J. Watts, J. Sarasa, F. J. Loge and A. L. Teel, Oxidative and reductive pathways in manganese-
511 catalyzed Fenton's reactions, *J. Environ. Eng.*, 2005, 131, 158-164.
- 512 30 A. L.-T. Pham, F. M. Doyle and D. L. Sedlak, Inhibitory effect of dissolved silica on H₂O₂
513 decomposition by iron(III) and manganese(IV) oxides: Implications for H₂ O₂ -based in situ chemical
514 oxidation, *Environ. Sci. Technol.*, 2012, 46, 1055–1062.
- 515 31 M. Kamagate, M. Pasturel, M. Brigante and K. Hanna, Mineralization enhancement of pharmaceutical
516 contaminants by radical-based oxidation promoted by oxide-bound metal ions, *Environ. Sci. Technol.*,
517 2019, 54, 476-485.
- 518 32 S. Balgooyen, P. J. Alaimo, C. K. Remucal and M. Ginder-Vogel, Structural transformation of MnO₂
519 during the oxidation of bisphenol A, *Environ. Sci. Technol.*, 2017, 51, 6053-6062.
- 520 33 K. Lin, W. Liu and J. Gan, Oxidative removal of bisphenol A by manganese dioxide: efficacy, products,
521 and pathways, *Environ. Sci. Technol.*, 2009, 43, 3860-3864.

- 522 34 J. Huang, S. Zhong, Y. Dai, C.-C. Liu and H. Zhang, Effect of MnO₂ phase structure on the oxidative
523 reactivity toward bisphenol A degradation, *Environ. Sci. Technol.*, 2018, 52, 11309–11318.
- 524 35 S. Balgooyen, G. Campagnola, C. K. Remucal and M. Ginder-Vogel, Impact of bisphenol A influent
525 concentration and reaction time on MnO₂ transformation in a stirred flow reactor, *Environ. Sci.*
526 *Process. Impacts.*, 2019, 21, 19–27.
- 527 36 R. M. McKenzie, The synthesis of birnessite, cryptomelane, and some other oxides and hydroxides of
528 manganese, *Mineral. Mag.*, 1971, 38, 493-502.
- 529 37 Q. Sun, P. X. Cui, T. T. Fan, S. Wu, M. Zhu, M. E. Alves, D. M. Zhou and Y. J. Wang, Effects of Fe
530 (II) on Cd (II) immobilization by Mn (III)-rich δ -MnO₂, *Chem. Eng. J.*, 2018, 353, 167-175.
- 531 38 A. A. Simanova, K. D. Kwon, S. E. Bone, J. R. Bargar, K. Refson, G. Sposito and J. Peña, Probing the
532 sorption reactivity of the edge surfaces in birnessite nanoparticles using nickel (II), *Geochim.*
533 *Cosmochim. Acta.*, 2015, 164, 191-204.
- 534 39 Y. Wu, M. Passananti, M. Brigante, W. Dong and G. Mailhot, Fe (III)–EDDS Complex in Fenton and
535 photo-Fenton processes: From the radical formation to the degradation of a target compound, *Environ.*
536 *Sci. Pollut. Res.*, 2014, 21, 12154–12162.
- 537 40 J. Mullin and J. Riley, The colorimetric determination of silicate with special reference to sea and
538 natural waters, *Anal. Chim. Acta.*, 1955, 12, 162-176.
- 539 41 V. Ruiz-Calero and M. T. Galceran, Ion chromatographic separations of phosphorus species: a review,
540 *Talanta.*, 2005, 66, 376-410.
- 541 42 Q. Li, R. Pokharel, L. Zhou, M. Pasturel and K. Hanna, Coupled effects of Mn(II), pH and anionic
542 ligands on the reactivity of nanostructured birnessite, *Environ. Sci. Nano.*, 2020, 7, 4022-4031.
- 543 43 J. Im, C. W. Prevatte, S. R. Campagna and F. E. Löffler, Identification of 4-hydroxycumyl alcohol as
544 the Major MnO₂-mediated bisphenol A transformation product and evaluation of its environmental
545 fate, *Environ. Sci. Technol.*, 2015, 49, 6214-6221.
- 546 44 H. Zhang, W. R. Chen and C. H. Huang, Kinetic modeling of oxidation of antibacterial agents by
547 manganese oxide, *Environ. Sci. Technol.*, 2008, 42, 5548-5554.

548 45 W. Stumm and J. J. Morgan, Aquatic chemistry: Chemical equilibria and rates in natural waters, John
549 Wiley & Sons., 2012.

550 46 S. Baral, C. Lume-pereira, E. Janata and A. Henglein, Chemistry of colloidal manganese dioxide. Part 2.
551 Reaction with O₂-and H₂O₂ (Pulse radiolysis and stop flow studies), J. Phys. Chem., 1985, 89, 5779-
552 5783.

553 47 D. B. Broughton and R. L. Wentworth, Mechanism of decomposition of hydrogen peroxide solutions
554 with manganese dioxide. I, J. Am. Chem. Soc., 1947, 69, 741–744.

555 48 J. P. Lefkowitz, A. A. Rouff and E. J. Elzinga, Influence of pH on the reductive transformation of
556 birnessite by aqueous Mn(II), Environ. Sci. Technol., 2013, 47, 10364-10371.

557 49 E. J. Elzinga, Reductive transformation of birnessite by aqueous Mn(II), Environ. Sci. Technol., 2011,
558 45, 6366-6372.

559 50 Q. Wang, P. Yang and M. Zhu. Structural Transformation of Birnessite by Fulvic Acid under Anoxic
560 Conditions, *Environ. Sci. Technol.*, 2018, **52**, 1844–1853.

561 51 H. Yin, Y. Zhou, J. Xu, S. Ai, L. Cui and L. Zhu, Amperometric biosensor based on tyrosinase
562 immobilized onto multiwalled carbon nanotubes-cobalt phthalocyanine-silk fibroin film and its
563 application to determine bisphenol A, *Anal. Chim. Acta.*, 2010, 659, 144-150.

564 52 H. Yin, Y. Zhou, L. Cui, X. Liu, S. Ai and L. Zhu, Electrochemical oxidation behavior of bisphenol A at
565 surfactant/layered double hydroxide modified glassy carbon electrode and its determination, *J. Solid
566 State Electrochem.*, 2011, 15, 167-173.

567 53 Ş. U. Karabiberoglu, Sensitive voltammetric determination of bisphenol A based on a glassy carbon
568 electrode modified with copper oxide-zinc oxide decorated on graphene oxide, *Electroanalysis.*, 2019,
569 31, 91-102.

570 54 H. Chenga, T. Yang, J. Jiang, X. Lu, P. Wang and J. Ma, Mn²⁺ effect on manganese oxides (MnO_x)
571 nanoparticles aggregation in solution: Chemical adsorption and cation bridging, *Environ. Pollut.*,
572 2020, 267, 115561.

573 55 H. Zhao, M. Zhu, W. Li, E. J. Elzinga, M. Villalobos, F. Liu, J. Zhang, X. Feng and D. L. Sparks, Redox
574 Reactions between Mn (II) and Hexagonal Birnessite Change its Layer Symmetry, *Environ. Sci.*
575 *Technol.*, 2016, **50**, 1750-1758.

576 56 S. M. Webb, G. J. Dick, J. R. Bargar and B. M. Tebo, Evidence for the presence of Mn(III)
577 intermediates in the bacterial oxidation of Mn(II), *Proc. Natl. Acad. Sci.*, 2005, 102, 5558-5563.

578 57 T. Takamatsu, M. Kawashima and M. Koyama, The role of Mn(II)-rich hydrous manganese oxide in the
579 accumulation of arsenic in lake sediments, *Water. Res.*, 1985, 19, 1029-1032.

580 58 W. Yao and F. J. Millero, Adsorption of phosphate on manganese dioxide in seawater, *Environ. Sci.*
581 *Technol.*, 1996, 30, 536-541.

582 59 P. Yang, K. Wen, K. A. Beyer, W. Xu, Q. Wang, D. Ma, J. Wu and M. Zhu, Inhibition of Oxyanions on
583 Redox-driven Transformation of Layered Manganese Oxides, *Environ. Sci. Technol.*, 2021, 55, 3419-
584 3429.

585 60 S. Mustafa, M. I. Zaman and S. Khan, pH effect on phosphate sorption by crystalline MnO₂, *J. Colloid*
586 *Interface Sci.*, 2006, 301, 370-375.

587 61 L. S. Balistrieri and T. T. Chao, Adsorption of selenium by amorphous iron oxyhydroxide and
588 manganese dioxide, *Geochim. Cosmochim. Acta.*, 1990, 54, 739-751.

589 62 S. Taujale and H. Zhang, Impact of interactions between metal oxides to oxidative reactivity of
590 manganese dioxide, *Environ. Sci. Technol.*, 2012, 46, 2764-2771.

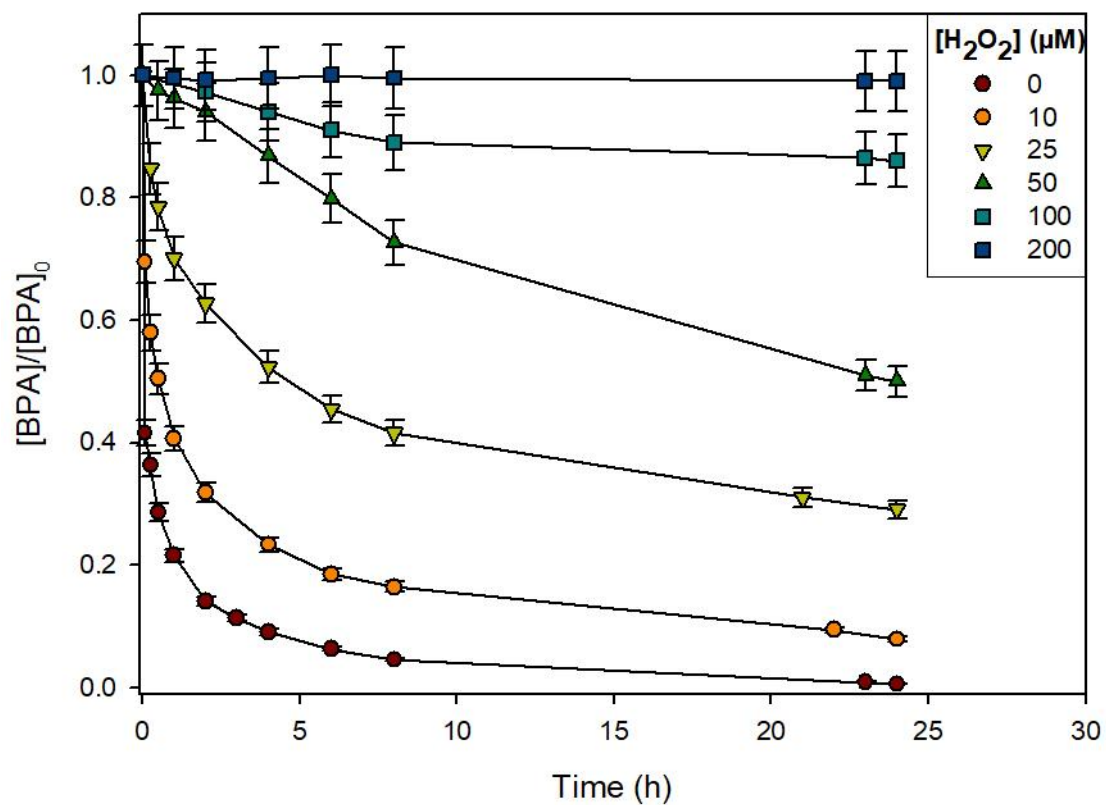
591 63 M. Yu, X. He, B. Xi, Y. Xiong, Z. Wang, D. Sheng, L. Zhu and X. Mao, Dissolved Silicate Enhances
592 the Oxidation of Chlorophenols by Permanganate: Important Role of Silicate-Stabilized MnO₂ Colloids,
593 *Environ. Sci. Technol.*, 2020, 54, 10279–10288.

594 64 C. K. Sharma, C. C. Chusuei, R. Clérac, T. Möller, K. R. Dunbar and A. Clearfield, Magnetic property
595 studies of manganese–phosphate complexes, *Inorg. Chem.*, 2003, 42, 8300-8308.

596 65 G. Friedl, B. Wehrli and A. Manceau, Solid phases in the cycling of manganese in eutrophic lakes: New
597 insights from EXAFS spectroscopy, *Geochim. Cosmochim. Acta.*, 1997, 61, 275-290.

598

599



600

601

Figure 1. Effect of H_2O_2 concentration on the BPA removal at pH 6.5 at room temperature.

602

Experimental conditions: $[AB] = 345 \mu M$, $[BPA] = 25 \mu M$. H_2O_2/MnO_2 ratio = 0 - 0.6.

603

604

605

606

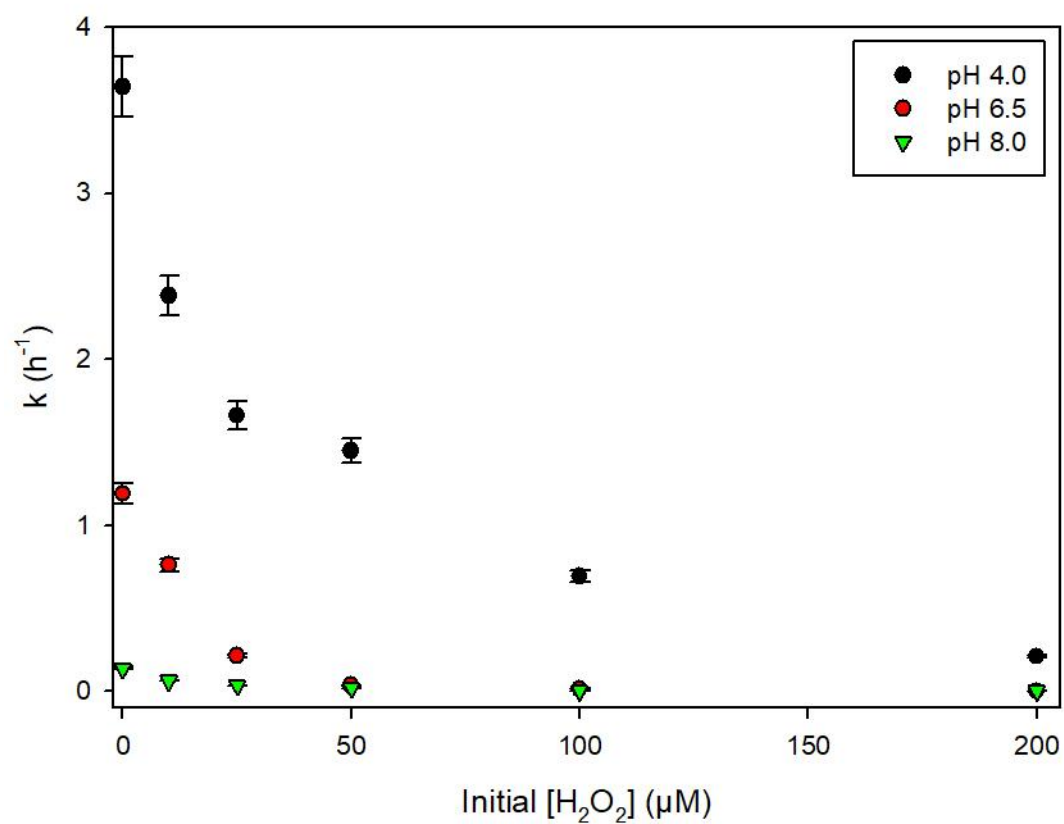
607

608

609

610

611

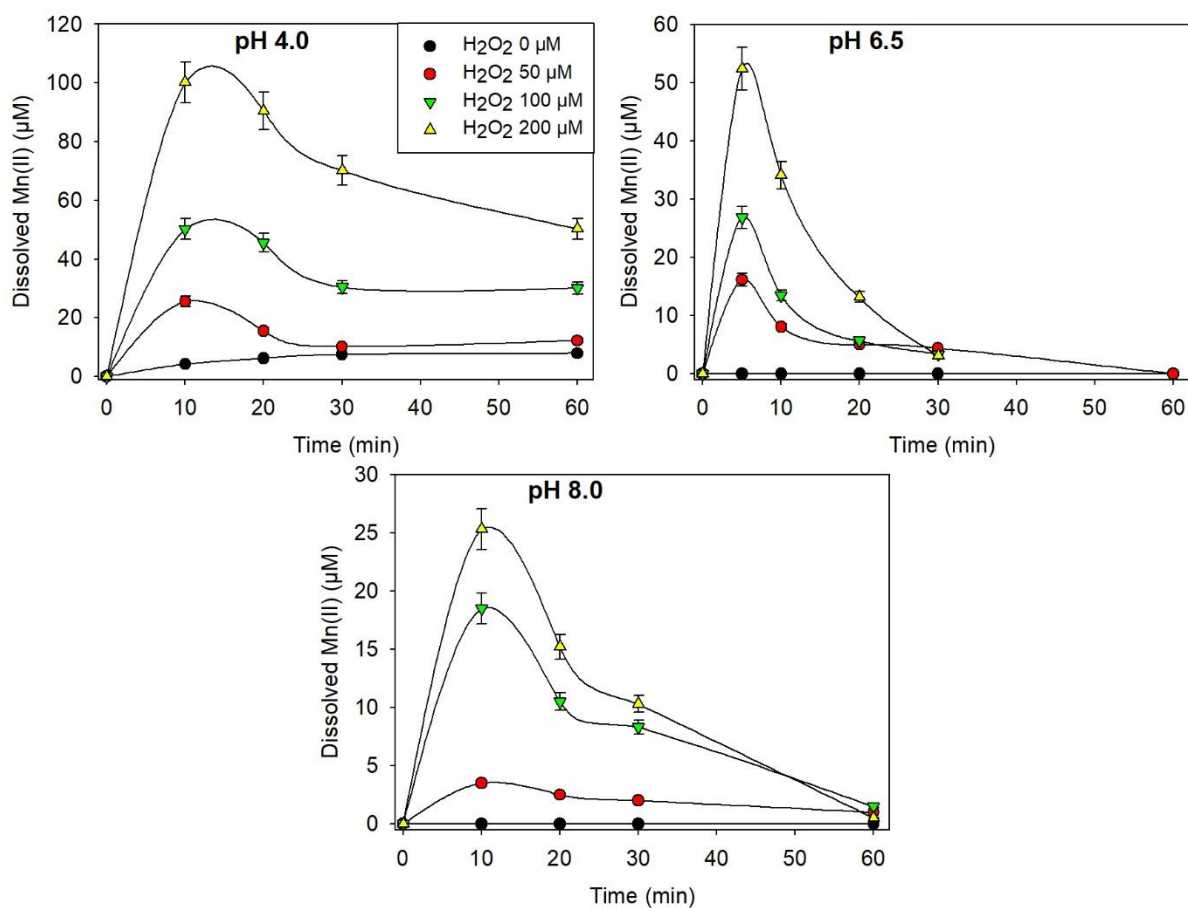


613

614 **Figure 2.** Removal rate constants (h⁻¹) of BPA as a function of H₂O₂ dose at three pH values
615 (4, 6.5 and 8). Experimental conditions: [AB] = 345 μM, [BPA] = 25 μM, [H₂O₂] = 0 - 200
616 μM. H₂O₂/MnO₂ ratio = 0 - 0.6.

617

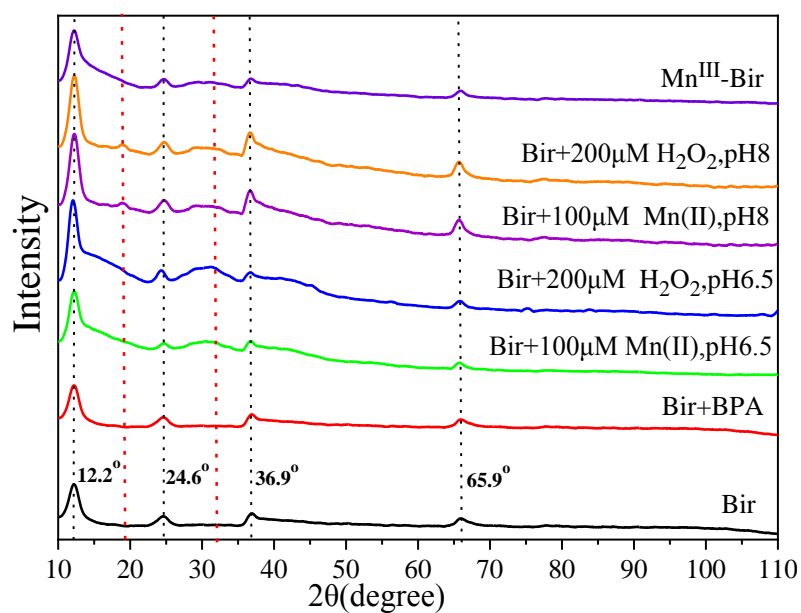
618



619
 620 **Figure 3.** Mn(II) formation under different H₂O₂ concentrations and pH 4.0, 6.5 and 8.0.

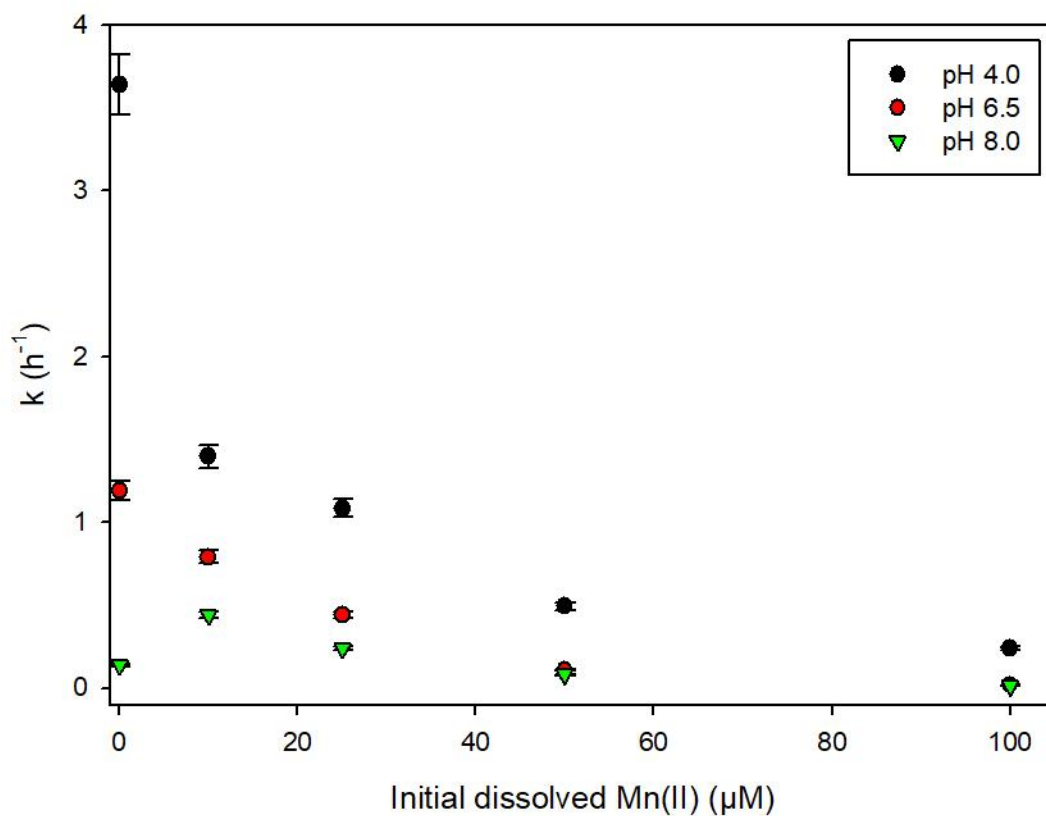
621 Experimental conditions: [AB] = 345 µM and [BPA] = 25 µM. H₂O₂/MnO₂ ratio = 0 - 0.6.

622
 623
 624
 625
 626
 627
 628
 629
 630
 631
 632



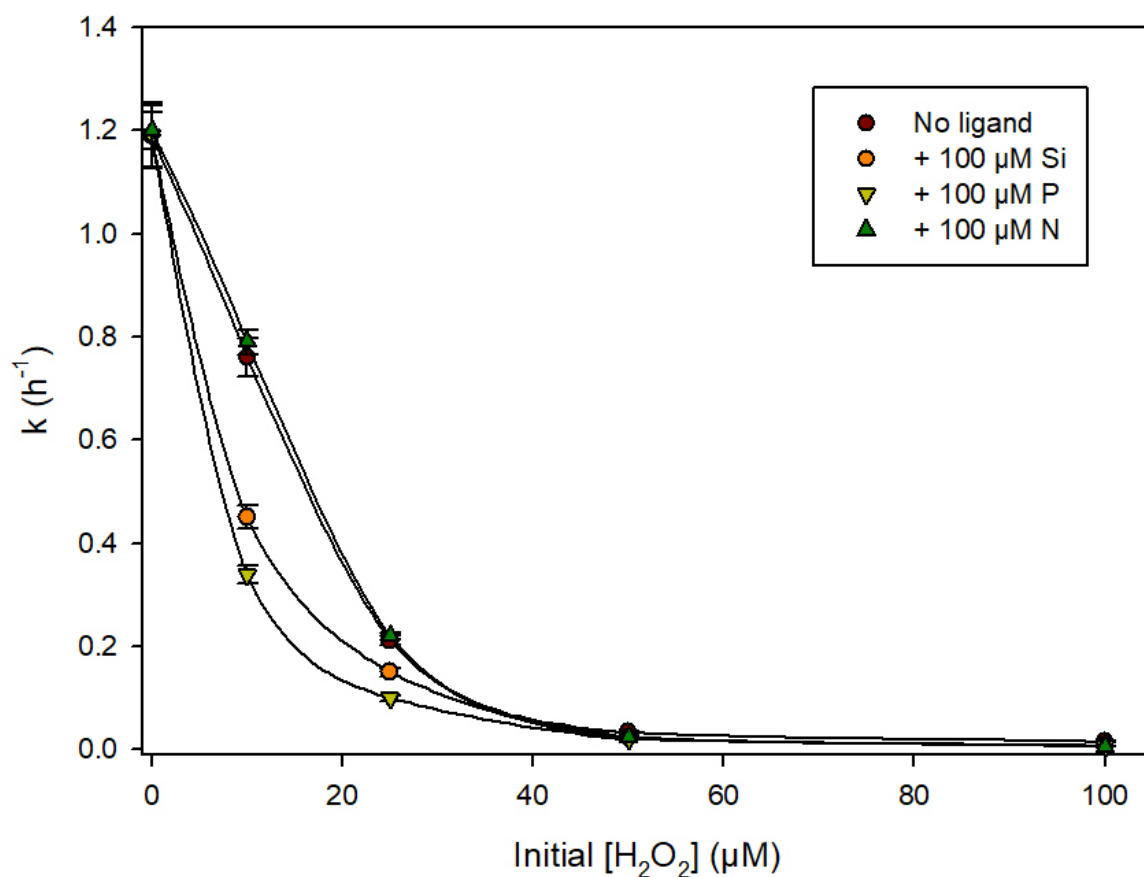
633
 634 **Figure 4.** XRD patterns of birnessite before and after reaction in the presence of H₂O₂ or
 635 Mn(II) (two pH values, 24 h of reaction time), and of Mn(III) rich Birnessite. The black
 636 dashed lines indicate the peaks of acid birnessite, while the red dashed lines indicate broad
 637 bands appeared in reacted samples. Experimental conditions: [AB] = 345 μM and [BPA] = 25
 638 μM. H₂O₂/MnO₂ ratio = 0.6. Mn(II)/MnO₂ ratio = 0.3.

639
 640
 641
 642
 643
 644
 645
 646
 647
 648



649
 650 **Figure 5.** Removal rate constants (h^{-1}) of BPA as a function of Mn(II) concentration at three
 651 pH values (4, 6.5 and 8). Experimental conditions: $[\text{AB}] = 345 \mu\text{M}$, $[\text{BPA}] = 25 \mu\text{M}$, $[\text{Mn(II)}]$
 652 $= 0 - 100 \mu\text{M}$.

653
 654
 655
 656
 657
 658
 659
 660
 661
 662



663

664

665

666 **Figure 6.** Removal rate constants (h^{-1}) of BPA as a function of H_2O_2 dose in absence or

667 presence of silicate (Si), nitrate (N) or phosphate (P): Experimental conditions: pH 6.5, [AB]

668 = 345 μM , [BPA] = 25 μM .; [Na_2SiO_3] = 100 μM ; [NaNO_3] = 100 μM ; [NaH_2PO_4] = 100 μM .

669 $\text{H}_2\text{O}_2/\text{MnO}_2$ ratio = 0 - 0.3.

670

671